

Introduction

Modern avalanche photodiodes (APDs or SiPMs) with high gain are excellent device candidates for the light readout from detectors used for the high energy physics experiments. The SiPMs are proposed as a main option for the light readout for Forward Wall Detector (FWD) at the BM@N [1] in the heavy-ion program at NICA [2]. Another application of SiPMs is the Projectile Spectator Detector (PSD) for the Compressed Baryonic Matter (CBM) project experimental program [3] for fixed target heavy ion collisions at FAIR in future.

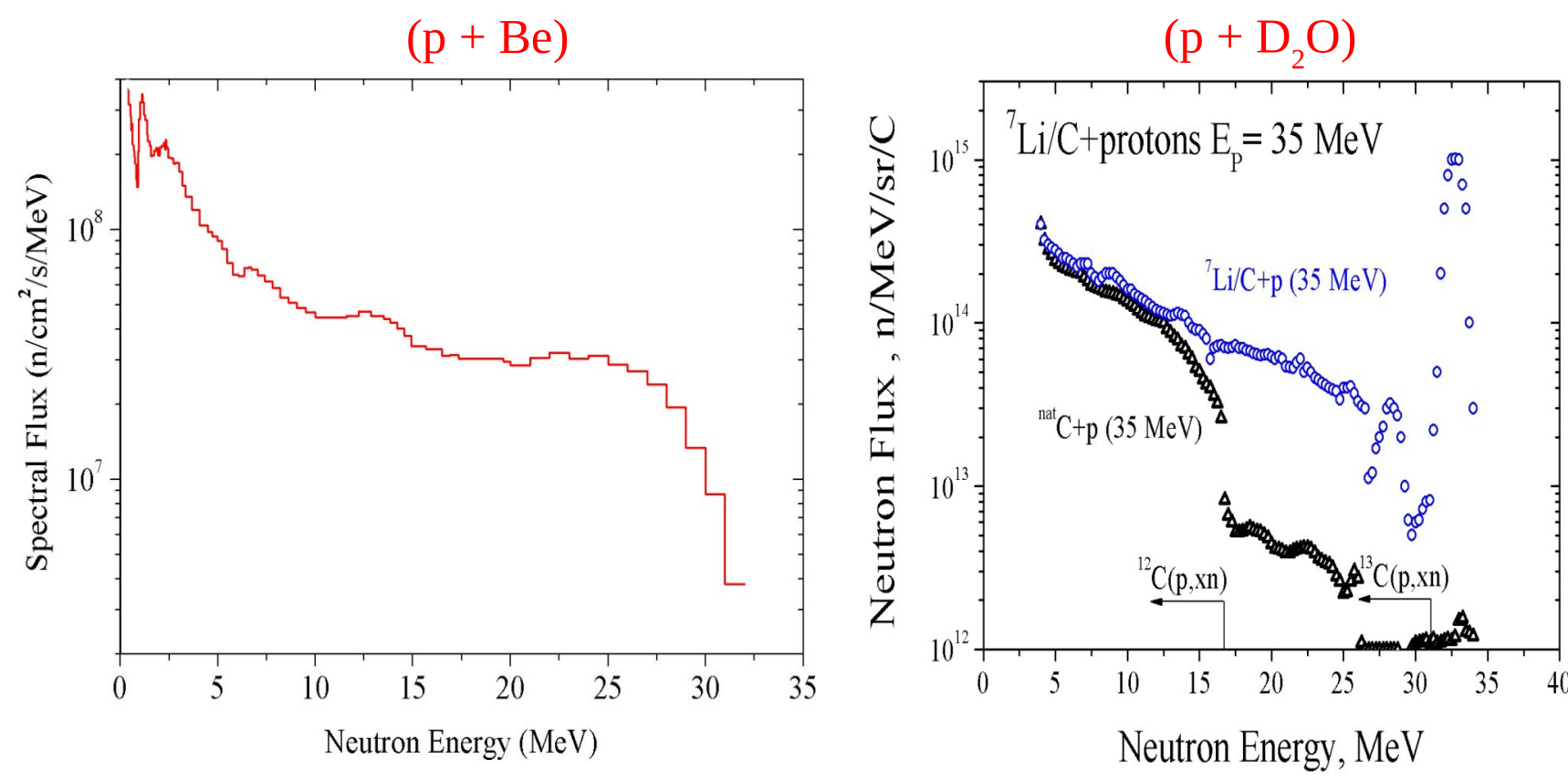
The main advantages of SiPMs are very compact sizes, low bias voltage, gain comparable to that for standard photomultiplier tubes (PMTs), relatively low price, insensitivity to magnetic field and absence of nuclear counter effect (due to the pixel structure). SiPMs have the following typical properties: pixel density about $10^4 - 2 \times 10^4 / \text{mm}^2$, size of $3 \times 3 \text{ mm}^2$, high dynamical range of 5–15000 p.h.e., photon detection efficiency of $\sim 15\%$, high counting rate of 10^7 Hz . The radiation hardness of SiPMs, especially to neutrons, plays a significant role for the detectors placed in the forward direction. For instance, according to FLUKA simulation [4] neutron flux near the beam hole might achieve 10^{12} neutrons/cm² for beam energy 4 A-GeV and 2 months of CBM run at the beam rate 10^8 ions per second [5] We report the results of the SiPMs radiation hardness study.

Four types of SiPM produced by Zecotec [6], Ketek [7], Hamamatsu [8], SENSL [9] were investigated to understand dependences of SiPMs radiation hardness on the manufacturing technology. The operational voltage and neutron fluence equivalent to neutrons with energy of 1 MeV for these types of SiPMs are given in table 1.

SiPM type	V _{bias} , V	Neutron fluence (1MeV), n/cm ²	Density impurities produced in W _{depl} , 1/cm ³	Temperature during irradiation, °C
Zecotec MSiPM-3N	88.5	$3.4 \pm 0.2 \cdot 10^{12}$	$2.47 \pm 0.65 \cdot 10^{10}$	22 ± 0.5
Ketek PM3350	23.5	$2.5 \pm 0.2 \cdot 10^{12}$	$1.31 \pm 0.43 \cdot 10^{11}$	22 ± 0.5
Hamamatsu S12572-010P	69.2	$3.9 \pm 0.5 \cdot 10^{12}$	$1.12 \pm 0.16 \cdot 10^{12}$	22 ± 0.5
SENSL uF B30020	25.0	$4.2 \pm 0.2 \cdot 10^8$	$4.49 \pm 0.12 \cdot 10^{11}$	23.1 ± 0.2

Cyclotron U120M facility

The SiPMs were irradiated using quasi-monoenergetic 35 MeV and “white-spectrum” secondary neutron beams from cyclotron facility U120M at NPI of ASCR, Řež. The setup for the beam fluence control and measurements of the irradiated SiPMs properties is described in [10].

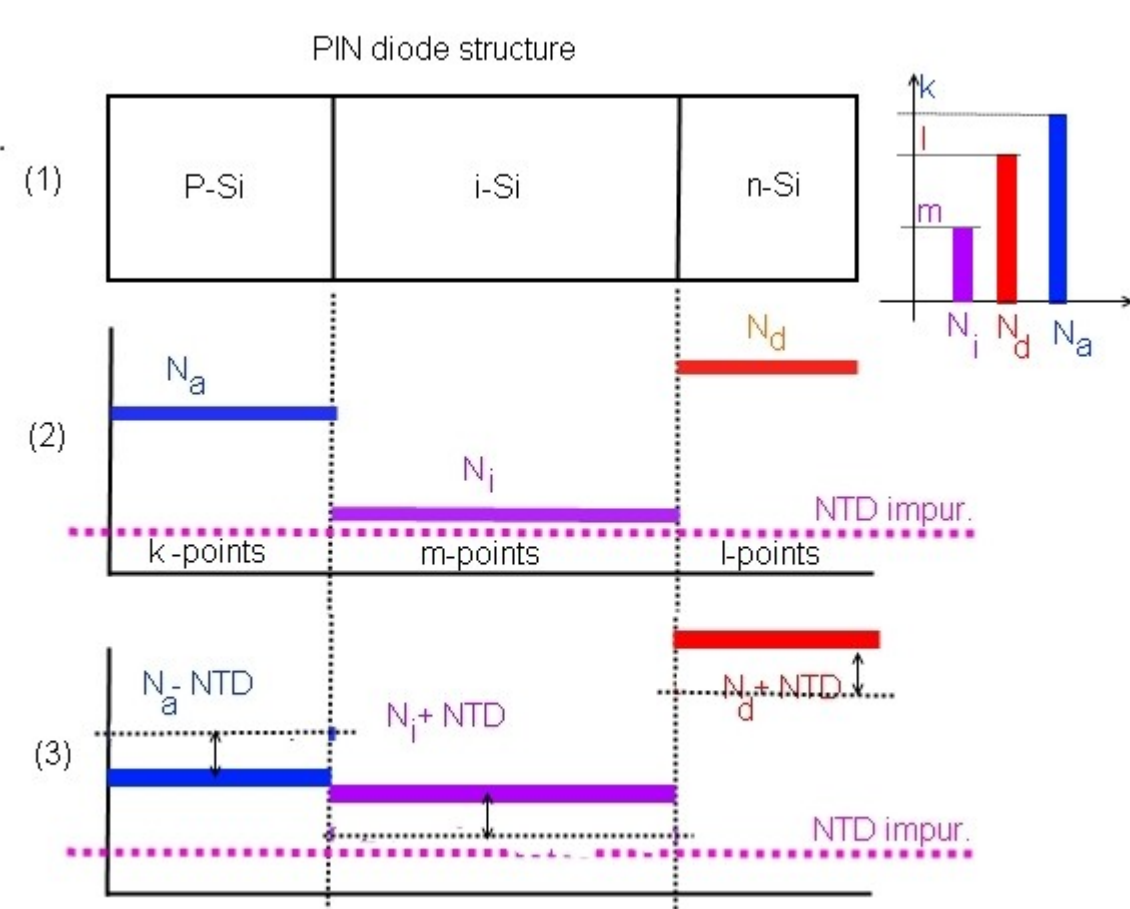


accelerated ions	energy [MeV]	extracted currents [μA]
H	6 - 38	15 - 35
H ⁺	6 - 38	3
d ⁺	11 - 20	3
³ He ²⁺	16 - 55	3
⁴ He ²⁺	22 - 40	3

Mono-energetic 20-37 MeV
(p+⁷Li) source: $3 \times 10^9 \text{ [n/cm}^2\text{/s]}$

Maximal flux:
(p+Be) source: $\sim 10^8 - 10^9 \text{ [n/cm}^2\text{/s]}$
(p+D₂O) source: $\sim 10^{11} \text{ [n/cm}^2\text{/s]}$

Change of Si doping by neutrons



It is based on the conversion of the Si-30 isotope into phosphorus atom by neutron absorption:



Neutrons continue to pass through the silicon, more and more phosphorus atoms are produced by transmutation, therefore, the doping becomes more and more strongly n-type.

HAMAMATSU

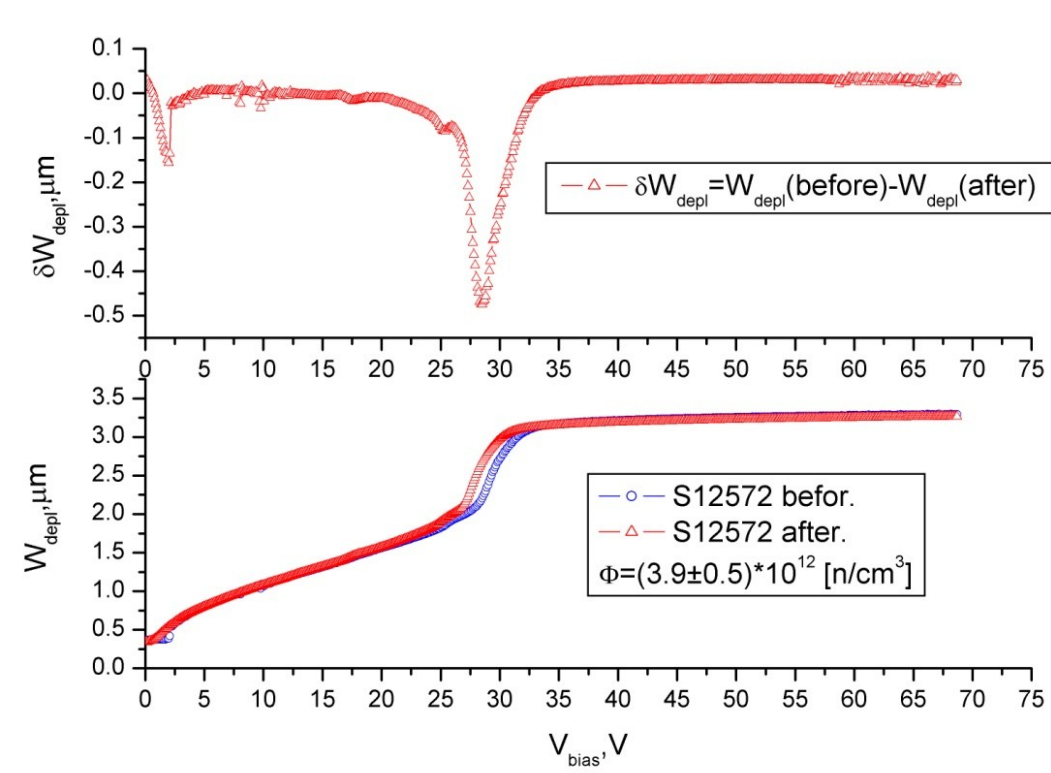


Fig. 1.1 Depletion width vs. V_{bias}

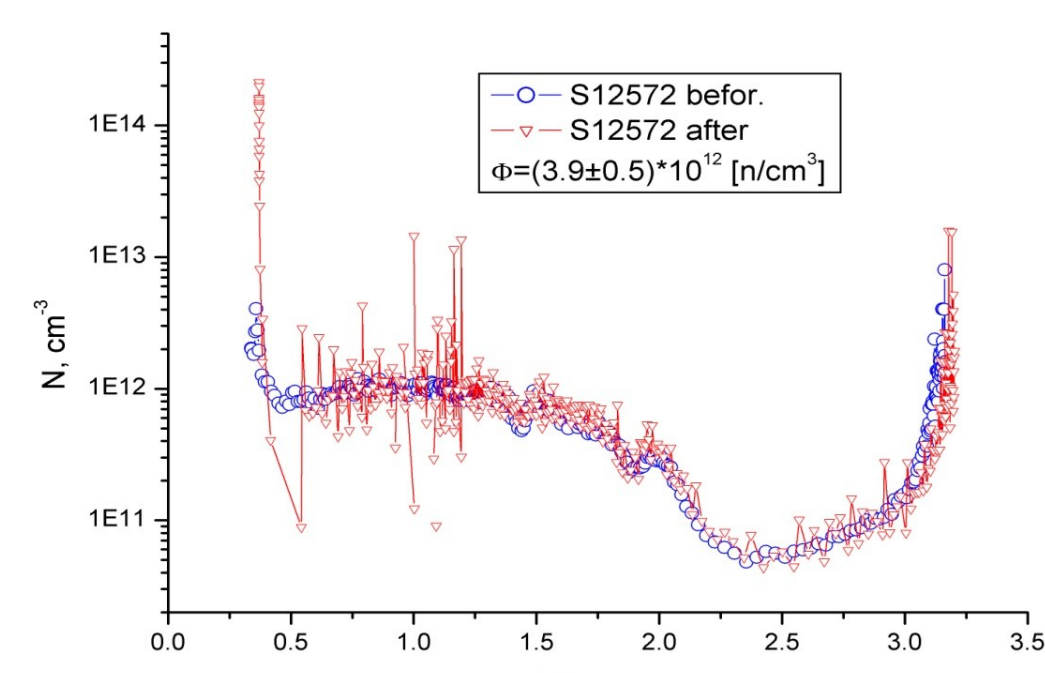


Fig. 1.2 Impurities produced in depletion region

Internal structure of HAMAMATSU changed more near surface, that can decrease sensitivity for blue light. Moreover, after irradiation detector is depleted for higher voltages. It can decrease sensitivity for light of long wavelength.

After first irradiation time of time to concentration ratio change not so strong as from beginning. Specific region from f_1 to f_2 was observed, where noise increase more than for other frequencies.

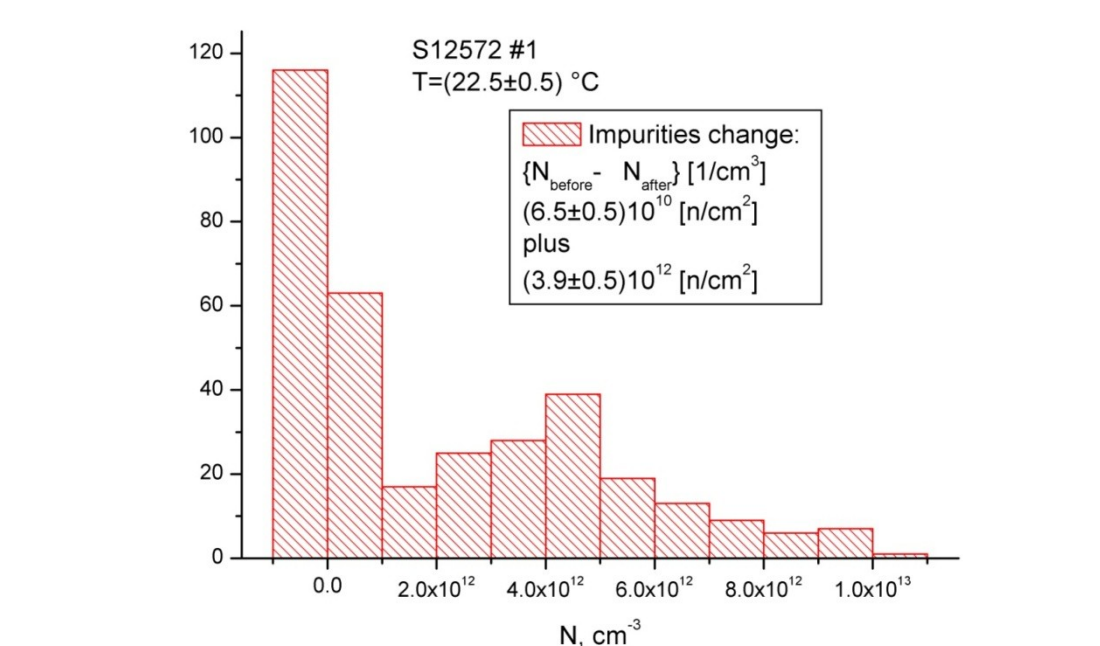


Fig. 1.3 The change of impurities after irradiation

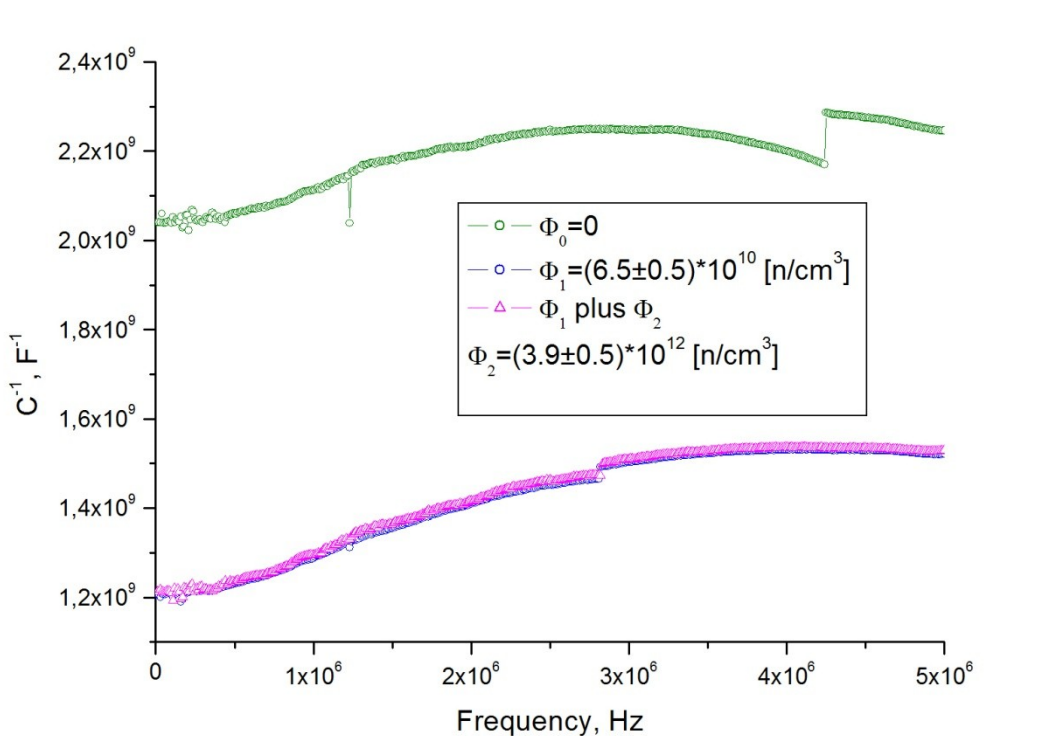


Fig. 1.4 Capacitance versus frequency

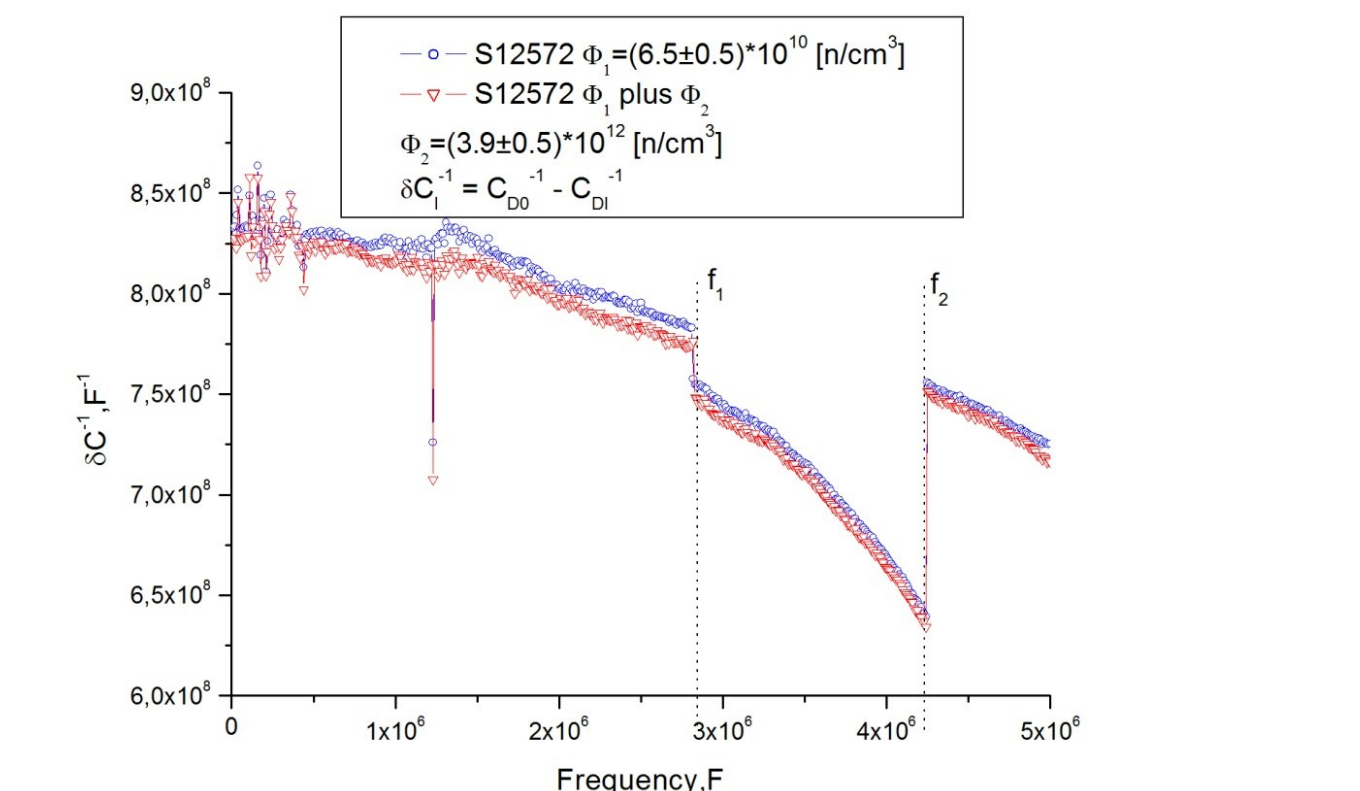


Fig. 1.5 Variation of capacitance before and after irradiation

KETEK

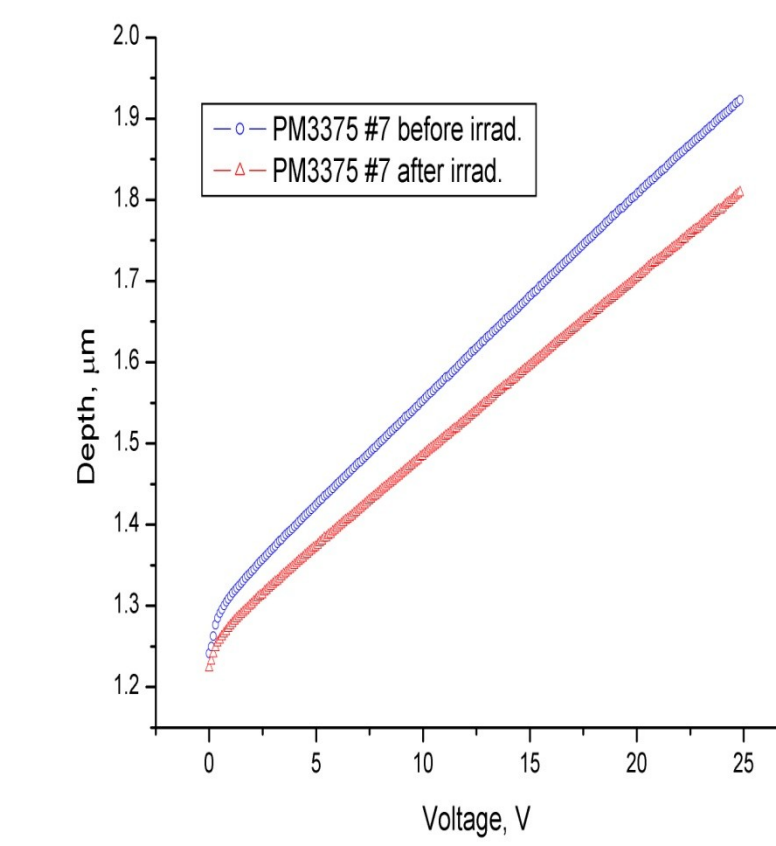


Fig. 2.1 Depletion width vs. V_{bias}

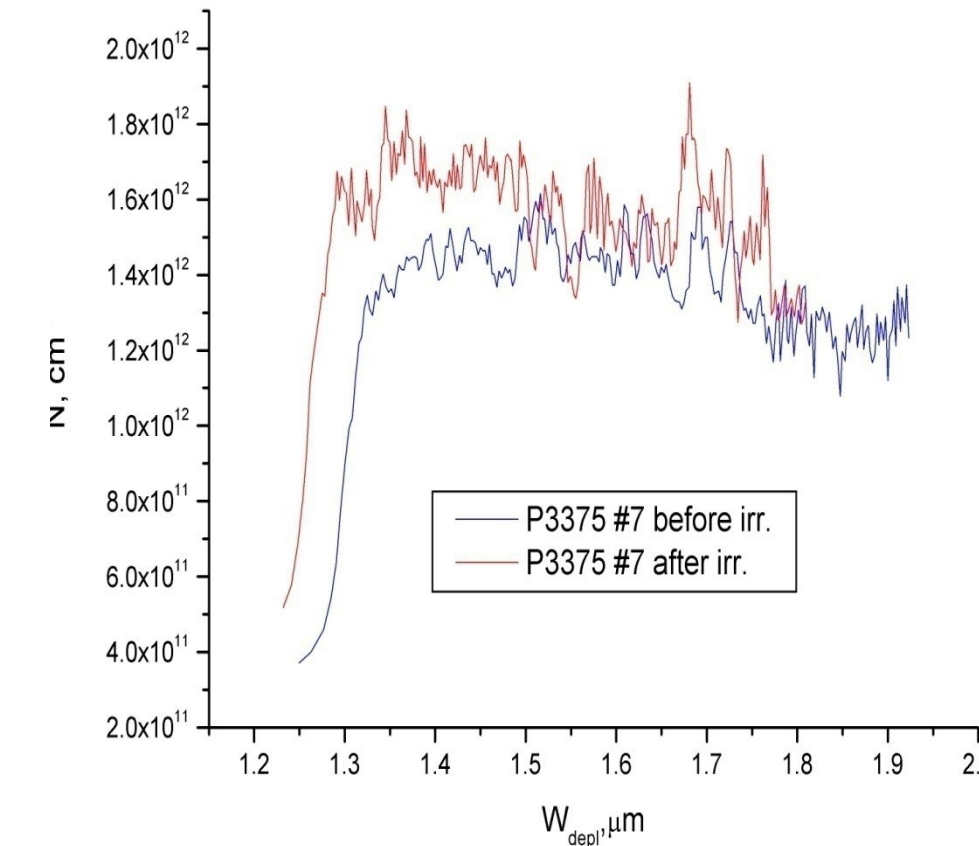


Fig. 2.2 Impurities produced in depletion region

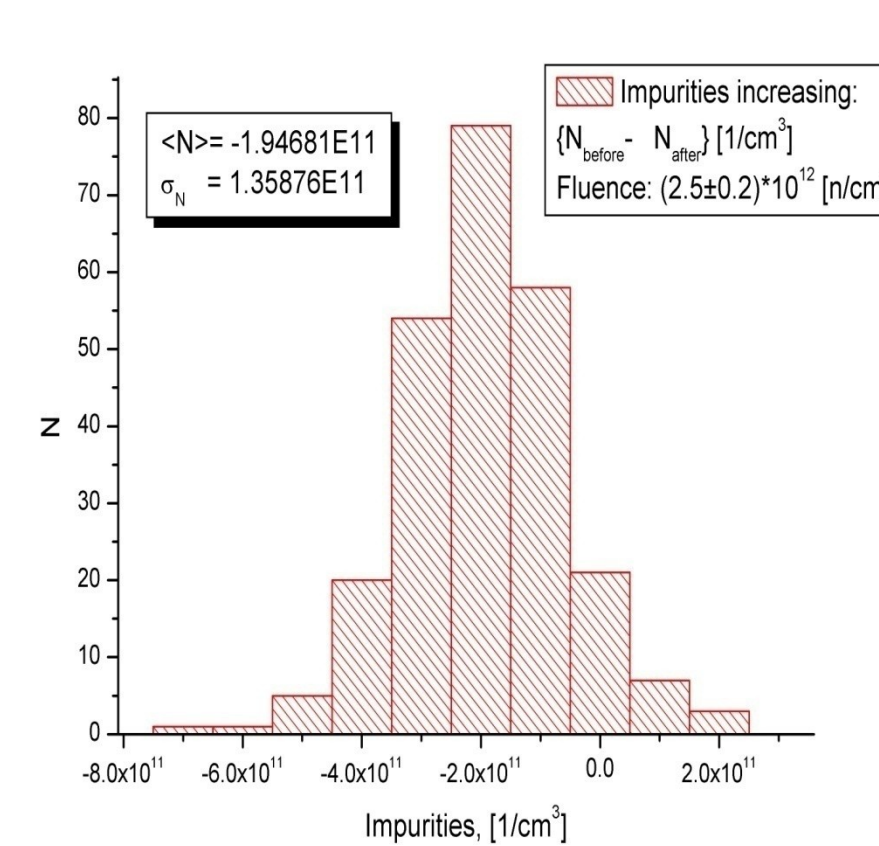


Fig. 2.3 The change of impurities after irradiation

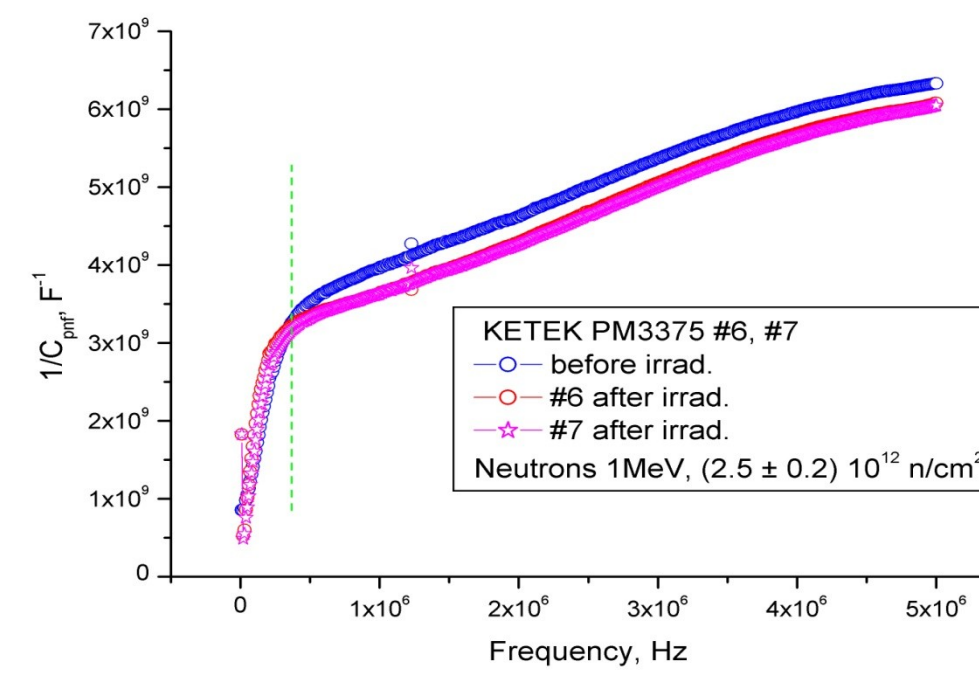


Fig. 2.4 Capacitance versus frequency

Internal resistance of KETEK SiPM decreases after irradiation that can be observed on Fig. 2.1 as depletion region shortening for the same voltages as before irradiation.

Generation-recombination noise $\delta < N_t^2 >$ depends on characteristics in Fig. 2.4 $\delta < N_t^2 > / N_t \sim (4\tau_n / (1 + (\omega\tau_n)^2))$; $\tau_n / N_t \sim 1/C(\omega)$; where N_t - average number of carriers from traps, τ_n - carrier lifetime; $\omega = 2\pi f$; f - frequency [12,13].

Generation-recombination noise decreases for low frequency, but increases for high frequency.

We use KETEK SiPM for readout scintillator's hodoscopes during neutron beam test. Decrease of gain and increase of internal noise due to neutrons were observed. Hodoscope system was developed in JINR for position monitoring of neutron beam for Cyclotron U120 in NPI Rez.

ZECOTEK

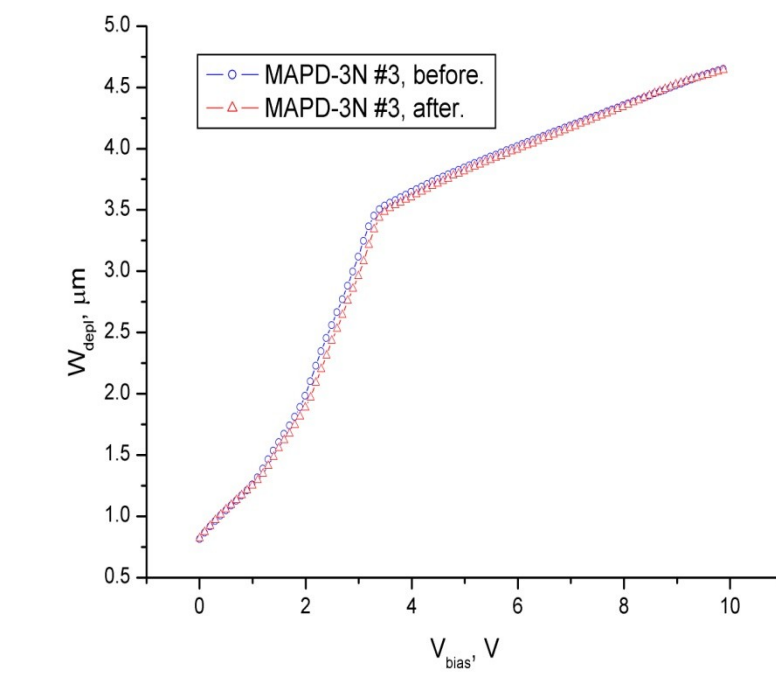


Fig. 3.1 Depletion width vs. V_{bias}

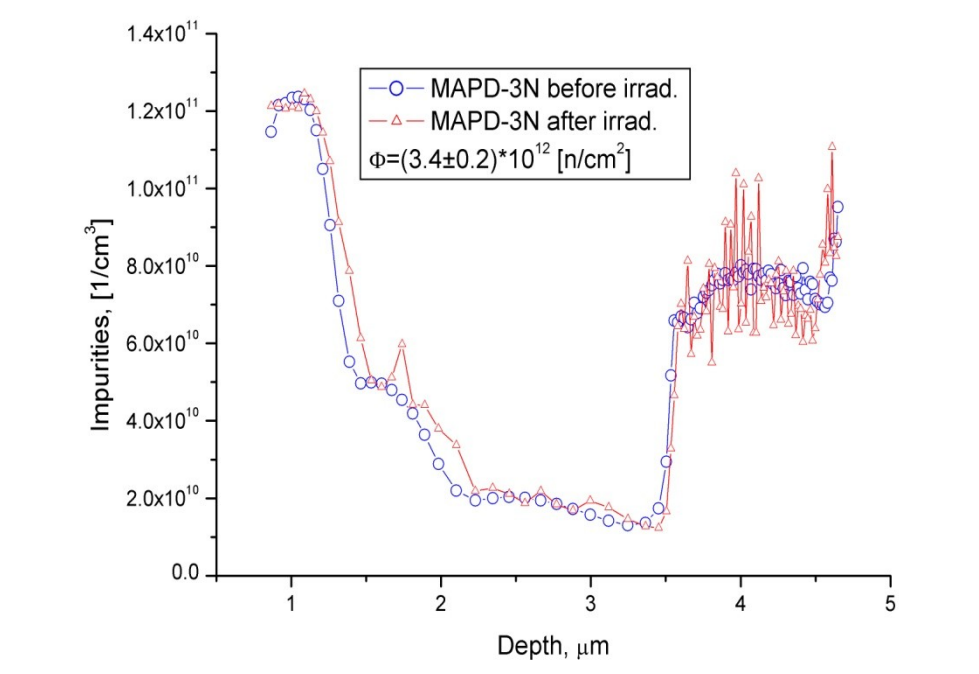


Fig. 3.2 Impurities produced in depletion region

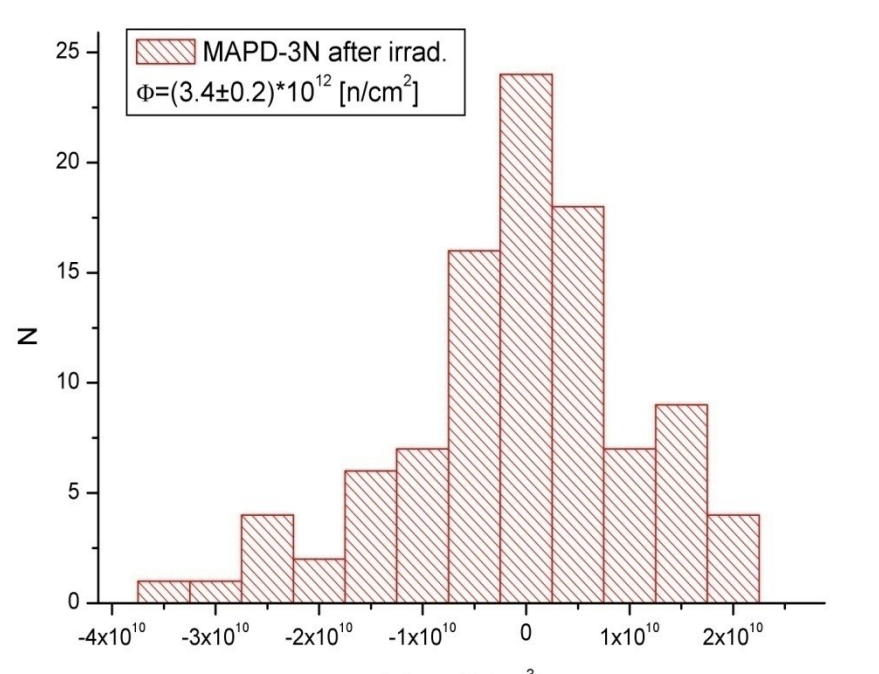


Fig. 3.3 The change of impurities after irradiation

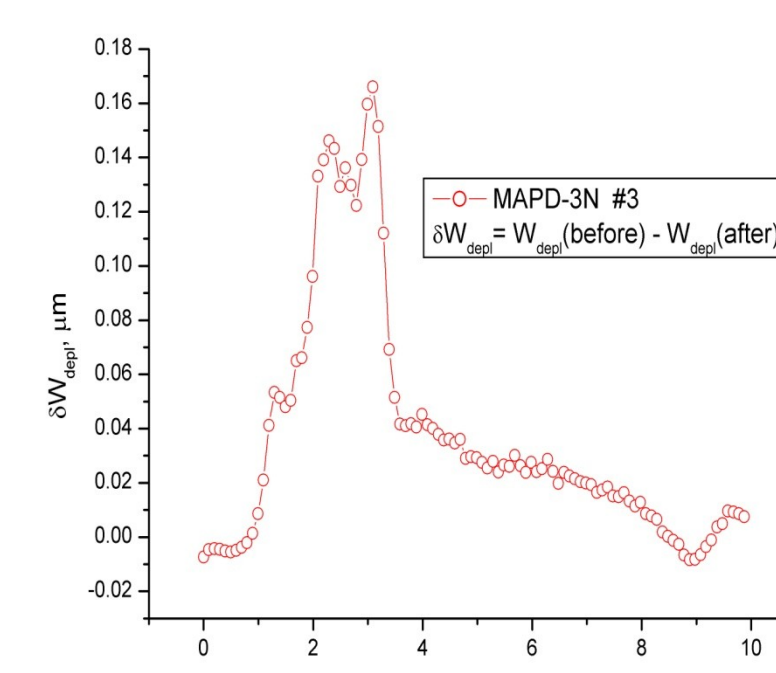


Fig. 3.4 Depletion width variation vs. V_{bias}

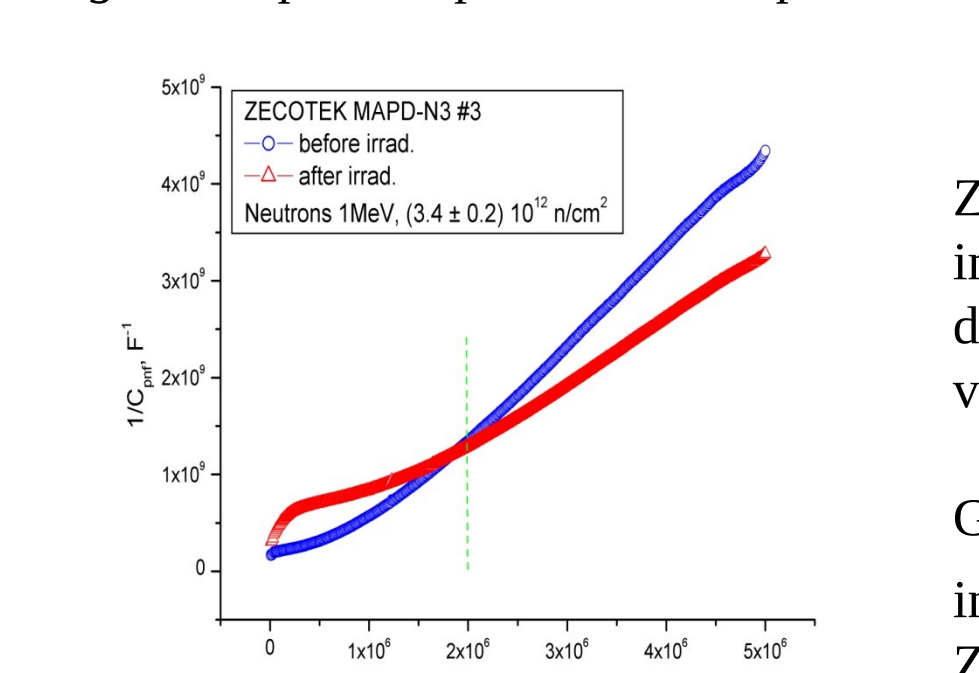


Fig. 3.5 Capacitance versus frequency

ZECOTEK has more symmetric change of impurities in depletion region. As a result, depletion region is more stable versus biasing voltage.

Generation-recombination noise $\delta < N_t^2 >$ increases for more high frequencies for ZECOTEK compared to KETEK.

SENSL SiPM

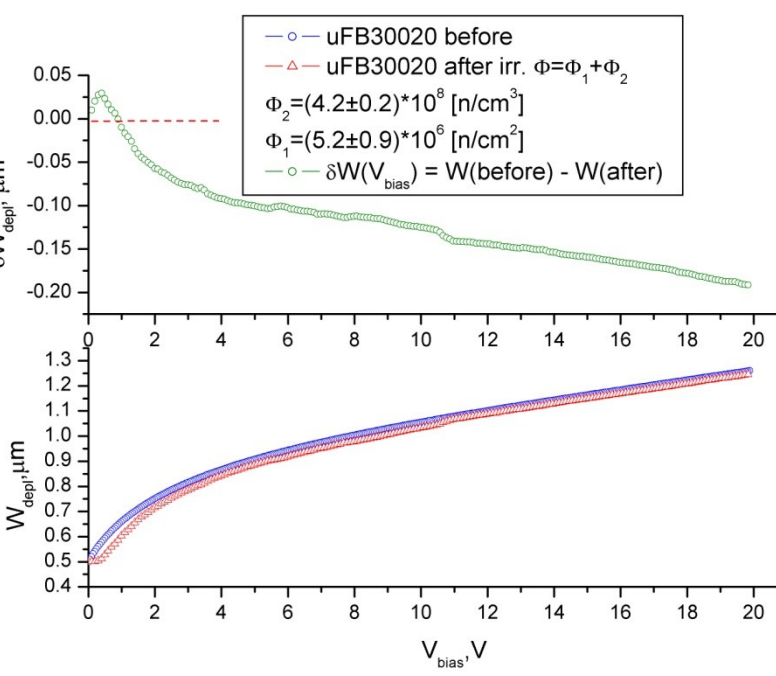


Fig. 4.1 Depletion width vs. V_{bias}

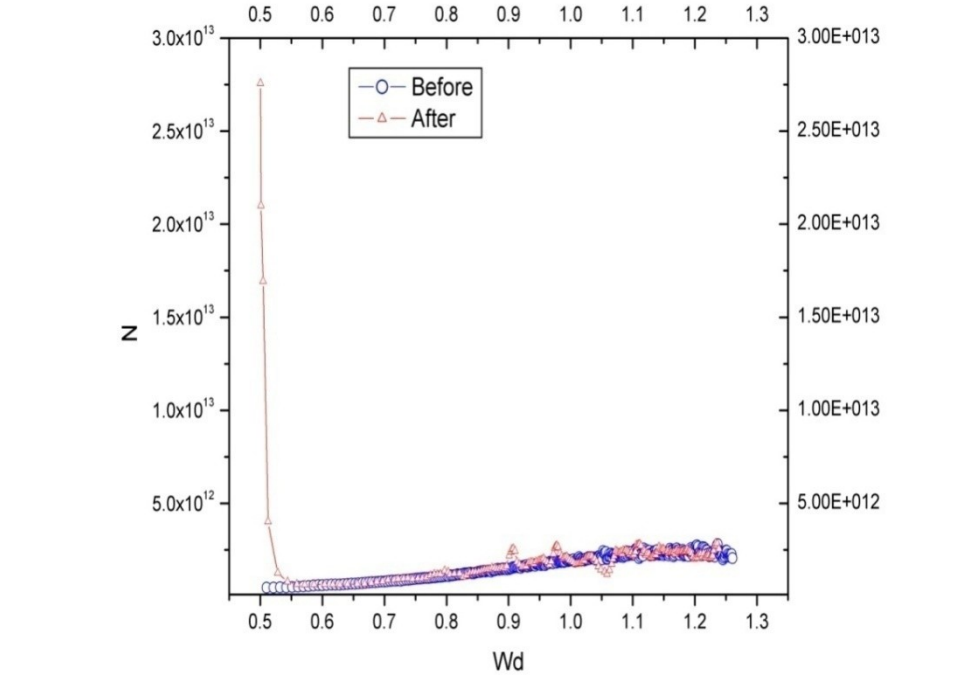


Fig. 4.2 Impurities produced in depletion region

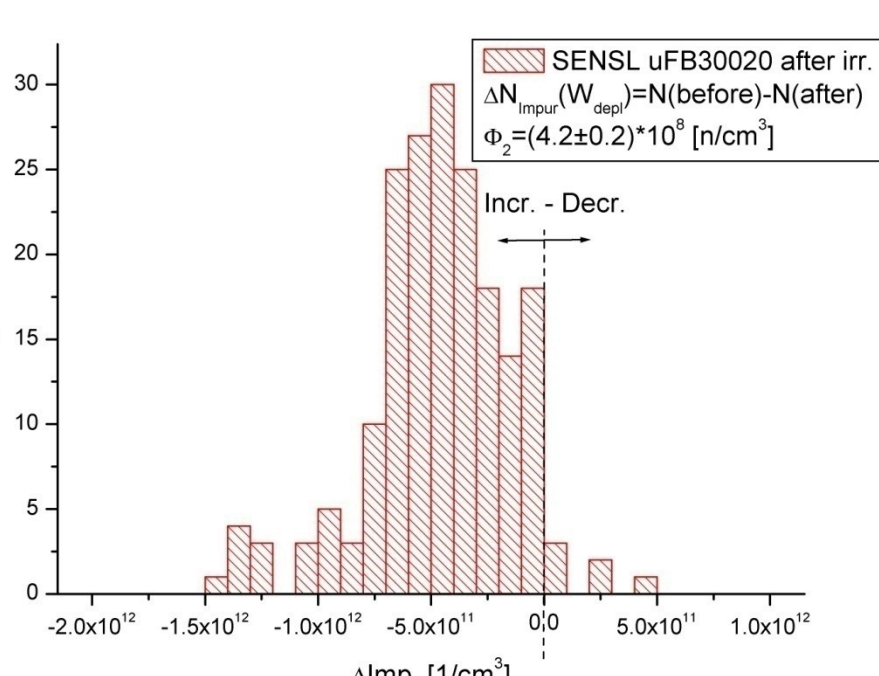


Fig. 4.3 The change of impurities after irradiation

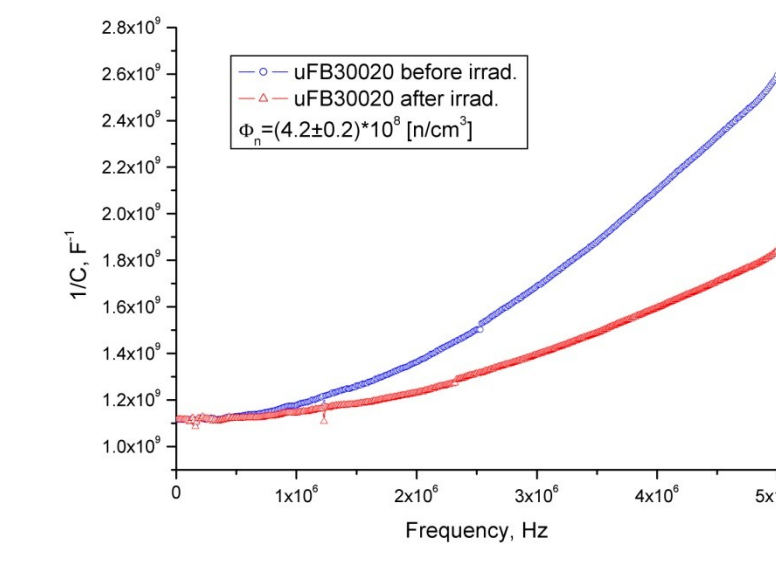


Fig. 4.4 Capacitance versus frequency

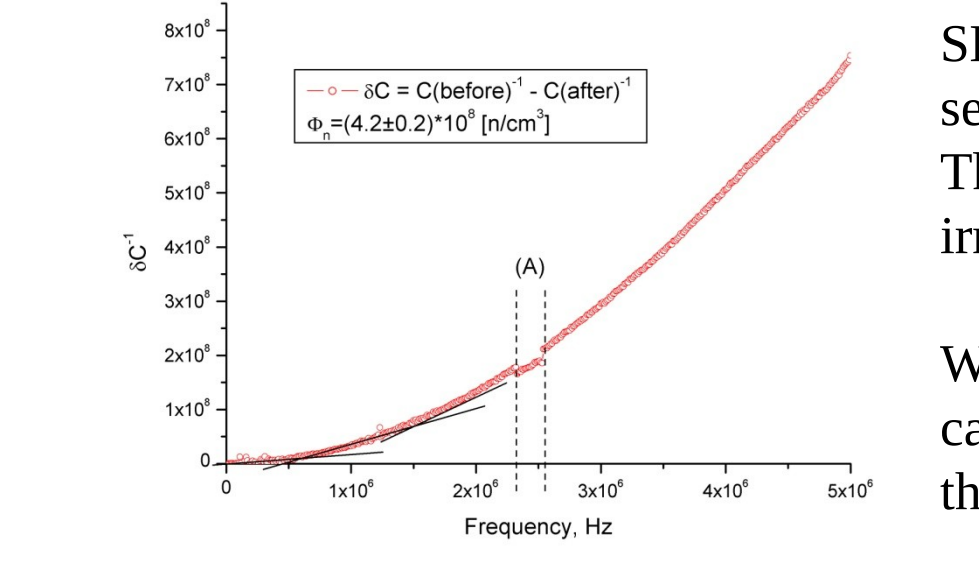


Fig. 4.5 Variation of capacitance before and after irradiation

SENSL compared to HAMAMATSU is more sensitive to irradiation in region near surface. Thermal neutrons flux was higher during irradiation of SENSL.

With help of neutron monitoring system calibrated for 1MeV neutrons, the part of thermal neutrons flux can be estimated.

Detector developed in JINR, Dubna was used for neutron monitoring. Generation-recombination noise increases homogeneity for all frequencies.

SUMMARY

- Influence of neutron irradiation on change of the concentration of internal doping inside Si active region was observed for all investigated detectors;
 - Depending on internal topology of detectors we observe two kinds of behavior after irradiation: 1) Detectors with simple topology such as KETEK and SENSL; 2) Detectors with more complex topology - HAMAMATSU and ZECOTEK;
 - Histograms of concentration show that HAMAMATSU, KETEK, SENSL SiPMs have more asymmetrical topology than ZECOTEK;
 - Ratio of lifetime to concentration of minority carriers (Tau/N) demonstrates different behaviors of recombination-generation processes after irradiation;
 - Difference in neutron fluence and number of generated impurities in active region for SENSL (Table 1) can be explained as result of higher fluxes of thermal neutrons during last irradiation;
- Conclusion:** We detect influence of neutron flux level on detector doping material. Different behavior of Tau/N ratio was observed, it can be detected independently by comparison of intrinsic noise spectrum of detectors after and before irradiation. It can be useful for development of readout electronics and improvement of detector technology.

Acknowledgments & References

The authors thank the NPI cyclotron and neutron generators staff for excellent beam conditions and service. This work was supported by the Ministry of Education, Youth and Sports of the Czech Republic project LM2011019 (CANAM) and project LG14004 (Cooperation Program between JINR and NPI in 2014-2015) and project LM2015049 (FAIR-CZ) and by RFBR under grant 16-02-00203 program.

- [1] Ablyazimov T. O. et al. (BM@N Collaboration). Conceptual Design Report of BM@N/ http://nca.jinr.ru/files/BM@N/BMN-CDR.pdf
- [2] Kekelidze V. D. et al. (NICA Collaboration). Design and Construction of Neutron-based Ion Collider Facility (NICA). Conceptual Design Report/ http://nca.jinr.ru.
- [3] Friman B., Hohn C., Kroll J., Leupold S., Randrup J., Rapp R. and Senger P. The CBM physics book: Compressed baryonic matter in laboratory experiments/Lect.Notes Phys. 2011. V.814. P.1.
- [4] Bohlen T. et al. The FLUKA Code: Developments and Challenges for High Energy and Medical Applications/ Nuclear Data Sheets. 2014. V.120. P.211.
- [5] Vasiliev T. A., Ladygin V. P. and Malakhov A. I. Energy dependence of the high p_T pion production and C₂ azimuthal correlation in heavy ion collisions in the experiments with fixed target/ Nucl. Phys. Proc. Suppl. B. 2011. V.219. P.312.
- [6] Zecotec WHITE PAPER MSiPM Photo-Detectors/ http://www.zecotec.com/media/MSiPM-WhitePaper-March-2011.pdf.
- [7] Ketek PM3350 Datasheet/ http://www.ketek.net/products/sipm/pm3350/
- [8] Hamamatsu S12572-010P Datasheet/ http://www.hamamatsu.com/jp/en/S12572-010P.html.
- [9] SenSL uFB30020 Datasheet http://sensl.com/downloads/ds/DS-MicroSeries.pdf
- [10] Kushpil V. et al. Investigation of SiPM radiation hardness for BM@N, Physics of Particles and Nuclei Letters, 2016, Vol.13, N1, pp120-126.
- [11] Mikhaylov V. et al. Radiation hardness tests of Avalanche Photodiodes for FAIR, NICA, and CERN SPS experiments, PoS (EPS-HEP2015) 282.
- [12] http://pos.sissa.it/archive/conferences/234/282/EPS-HEP2015_282.pdf
- [13] http://www.ee.buffalo.edu/faculty/mitin/Papers/VMitin_doc_1-20-10.pdf